

ORIGINAL ARTICLE

Topology Optimization of A Composites Frame Structure Considering Ply Orientation for Medium-Altitude Long-Endurance Unmanned Aerial Vehicle (MALE UAV)

I B Wiranto¹, S O Saraswati¹, I R Alfikri¹, Chairunnisa² and A Aribowo^{3,*}¹Research Center for Process and Manufacturing Industry Technology, BRIN, Indonesia²Research Center for Energy Conversion and Conservation, BRIN, Indonesia³Research Center for Aeronautics Technology, BRIN, Indonesia

ABSTRACT – This research employs the Finite element method to optimize the frame structure of a medium-altitude long-endurance unmanned aerial vehicle (MALE UAV). The material used in this study is a unidirectional carbon fiber stacked in a specific sequence. The topology optimization process was conducted to achieve a lightweight structure whilst maintaining its integrity. The design constraint was set to reduce 50% weight and minimize the strain energy. The benchmark phase was performed while considering a previously done study to validate the proposed method. The results of this study have successfully reduced 34% (0.581 kg) weight of the frame structure. The first failure prediction study using Hashin criterion shows the first failure occurred in the matrix of Ply-2 at 9000 N.

ARTICLE HISTORY

Received: 8 Sept 2022

Revised: 6 Oct 2022

Accepted: 8 Oct 2022

KEYWORDS

Topology optimization

MALE UAV

Carbon fiber

Finite element method

INTRODUCTION

Another strategy for reducing weight by maintaining strength in structural optimization is topology optimization (TO). Topology optimization is a sophisticated structural design technique that can produce the ideal structure configuration through appropriate material distribution while meeting certain load circumstances, performance requirements, and constraint requirements [1]. One of the common methods in topology optimization using Abaqus is shell elements, which bring the advantages of simple geometry and less mesh [2]. Every element are assigned to have mechanical properties and the optimization process works by removing some of those elements. The majority of the time, the aim is to increase structural integrity while lowering model volume or weight as a constraint. Minimizing strain energy in the model results in an increase in stiffness [3].

Topology optimization has been heavily used during the lightweight design to strike a compromise between weight reduction and meeting structural strength requirements [4]. The automotive and aerospace industries escalating usage of composite materials over the past few decades has created a need for increased production rates while upholding high-quality standards.

Points to consider while using carbon fiber are, compare to topology optimization with a fixed orientation, the element, patch, and ply orientation models can greatly enhance the overall stiffness (compliance) of structures under out-of-plane loadings. Concurrent optimization of the structural topology and anisotropic material for laminated composite structures was carried out by optimizing the laminate topology and fiber orientation simultaneously. Additionally, even when two sets of design variables (topological and orientation) are optimized concurrently, all optimization models are comparatively stable [5].

For the material qualities to be applied to the base structure, there are numerous alternatives. The method can be used to create composite sandwich structures as well as shell in-fill structures that are common in additive manufacturing processes using fused filament fabrication (FFF). The mechanical characteristics of a constant-density triangular honeycomb are taken into account for composite sandwich applications, where a low-density core is produced using the FFF additive manufacturing process [6].

The automotive and aerospace industries' escalating usage of composite materials over the past few decades has created a need for increased production rates while upholding high-quality standards. In order to meet this need, autoclave resin infusion technologies like resin transfer molding (RTM) and liquid resin infusion (LRI) have been created and further developed as quicker and more affordable manufacturing procedures than traditional hand lay-up of prepregs and autoclave processing. LRI is comparable to those produced by the prepreg technique [7].

Despite the fact that certain pertinent studies optimized topologies using the classical plate theory, it is also common to consider the layerwise theory. When evaluated using the conventional plate theory, laminate systems with enormous layer thicknesses are not anticipated to be very accurate [8].

By selecting materials and optimization techniques carefully, it is possible to reduce the structure's weight. The design of continuous fiber composite structures is restricted to simple geometries, such as sandwich panels with a constant

thickness or stiffened panels with evenly spaced, constant cross-section stiffeners, primarily due to costs and manufacturability constraints [3]. These days, composite materials are frequently used in the aerospace sector because of their distinct mechanical and physical properties. The use of polymer composite materials in the load-bearing components of an airplane fuselage allows the airframe to be lighter while simultaneously improving its aerodynamic performance [3].

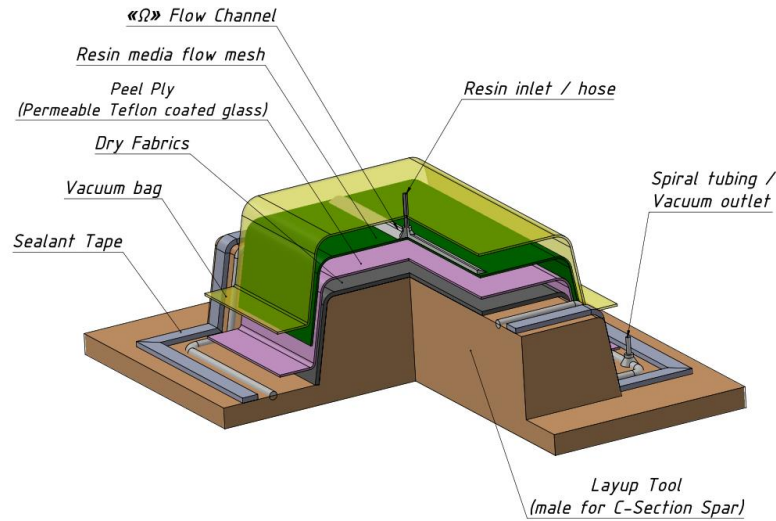


Figure 1. LRI process schematic representation [7]

Damage processes in composite laminates structure vary widely and are influenced by a variety of factors. For unidirectional fiber composites, the Hashin damage criterion interacts with many stress components to assess various fracture modes. Four failure modes are involved in the failure indices for the Hashin criteria that pertain to fiber and matrix failure. The quadratic interaction criterion between the various tractions has improved the Hashin criterion's capacity for prediction [9].

An intra-laminar damage criterion is used in the standard Abaqus calculation code to implement the growth forecast and the damage trajectory[10]. Transverse, longitudinal, and shear strength, as well as longitudinal and transverse tensile and compressive strength, serve as the input data for the Hashin criterion. There are various ways that anything might be damaged, such as when a fiber or matrix breaks under tension or compression. The quadratic nature of the Hashin criterion may be employed to account for the fit of the curve rather than mechanical behavior [11]. The general forms of Hashin criteria are as follows [2]:

1. Tensile fiber failure for $\sigma_{11} \geq 0$;
$$\left(\frac{\sigma_{11}}{X_T}\right)^2 + \frac{\sigma_{12}^2 + \sigma_{13}^2}{S_{12}^2} = \begin{cases} \geq 1 & \text{failure} \\ < 1 & \text{no failure} \end{cases} \quad (1)$$

2. Compressive fiber failure for $\sigma_{11} < 0$;
$$\left(\frac{\sigma_{11}}{X_C}\right)^2 = \begin{cases} \geq 1 & \text{failure} \\ < 1 & \text{no failure} \end{cases} \quad (2)$$

3. Tensile matrix failure for $\sigma_{22} + \sigma_{33} > 0$;
$$\frac{(\sigma_{22} + \sigma_{33})^2}{Y_T^2} + \frac{\sigma_{23}^2 - \sigma_{22}\sigma_{33}}{S_{23}^2} + \frac{\sigma_{12}^2 + \sigma_{13}^2}{S_{12}^2} = \begin{cases} \geq 1 & \text{failure} \\ < 1 & \text{no failure} \end{cases} \quad (3)$$

4. Compressive matrix failure for $\sigma_{22} + \sigma_{33} < 0$;
$$\left[\left(\frac{Y_C}{2S_{23}}\right)^2 - 1\right] \left(\frac{\sigma_{22} + \sigma_{33}}{Y_C}\right) + \frac{(\sigma_{22} + \sigma_{33})^2}{4S_{23}^2} + \frac{\sigma_{23}^2 - \sigma_{22}\sigma_{33}}{S_{23}^2} + \frac{\sigma_{12}^2 + \sigma_{13}^2}{S_{12}^2} = \begin{cases} \geq 1 & \text{failure} \\ < 1 & \text{no failure} \end{cases} \quad (4)$$

5. Interlaminar tensile failure for $\sigma_{33} > 0$;
$$\left(\frac{\sigma_{33}}{Z_T}\right)^2 = \begin{cases} \geq 1 & \text{failure} \\ < 1 & \text{no failure} \end{cases} \quad (5)$$

6. Interlaminar compression failure for $\sigma_{33} < 0$;
$$\left(\frac{\sigma_{33}}{Z_C}\right)^2 = \begin{cases} \geq 1 & \text{failure} \\ < 1 & \text{no failure} \end{cases} \quad (6)$$

where σ_{11} , σ_{22} , and σ_{33} denote general plane state of stress, S_{11} is a value of σ_{11} at longitudinal tensile or compressive failure, S_{22} is a value of σ_{22} at transverse tensile or compressive failure, S_{12} is the absolute value of σ_{12} at longitudinal shear failure, S_{23} is the absolute value of σ_{23} at transverse shear failure, Y_C is transverse compressive failure stress, and Y_T is transverse tensile failure stress.

In this study, a numerical approach based on finite element method (FEM) is applied to optimize a frame structure of medium-altitude long-endurance unmanned aerial vehicle (MALE UAV). The topological optimization and finite element analysis were done using a software, Abaqus FEA [10]. The objectives of this study are to reduce the weight of frame structure using topology optimization and to investigate the first failure that might be occurred in the optimized frame. The numerical validation process conducted on a squared design domain taken from the previous study [8]. The next process setup is within the Tosca optimization module. The topology optimization can minimize the strain energy in order to improve structural integrity, whereas the weight fraction is determined as a constraint design response which resulted in a light yet strong structure. The Hashin damage criterion is also implemented in this study to investigate the first failure of the frame structure. The first failure investigation was done by applying various loads to the frame structure until one of the Hashin criterion reach the value of 1. In conclusion, the optimization results show a lighter design of fuselage structure with a prediction of failure.

METHODOLOGY

In this study, topology optimization and ply failure prediction using Hashin criterion were conducted. It is common to normalize the physical properties of the material in the topology optimization problem. In this work, the stiffness properties of the anisotropic materials are normalized based on an isotropic material with an elastic modulus (E). The material that is used in this study has a thickness of 0.237 mm. The frame is made of 11 plies of unidirectional carbon-fiber prepreg shown in Figure 2.

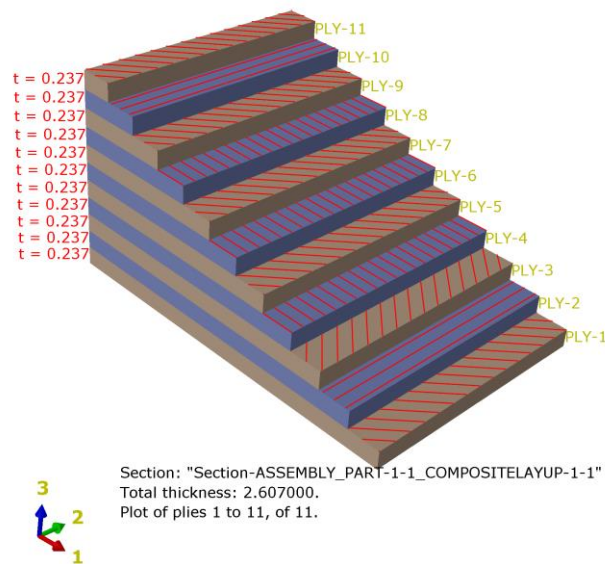


Figure 2. Frame stacking sequence representation.

Table 1. Stacking sequence of unidirectional composite used

Ply	Orientation (°)	Thickness (mm)
1	45	0.237
2	90	0.237
3	-45	0.237
4	0	0.237
5	45	0.237
6	0	0.237
7	45	0.237
8	0	0.237
9	-45	0.237
10	90	0.237
11	45	0.237

There are many combinations of stacking sequences to obtain different mechanical properties of carbon fiber materials. For this study, the stacking sequence for the frame can be seen in Table 1. Figure 2 shows the orientation of a stacked laminate composite. The value of 0° orientation angle (x-axis) is represented by red arrow (axis-1) and 90° orientation angle is represented by green arrow (axis-2).

The given material properties of unidirectional carbon fiber Hexcel W3G282-F593 [12] is limited to a single ply only (0.237 mm), hence the normalization of 11-ply unidirectional carbon fiber is performed at the start of the optimization.

The mechanical properties of 11-ply unidirectional carbon fiber generated from the normalization process are shown in Table 2.

Table 2. Normalized material properties of 11-ply unidirectional carbon fiber

	Density (ton/mm ³)	E ₁ (GPa)	E ₂ (GPa)	Nu ₁₂	G ₁₂ (GPa)	G ₁₃ (GPa)	G ₂₃ (GPa)
Carbon Fiber Unidirectional	1.6×10^{-9}	36	36	0.581	12.9	12.9	12.9

Note:

E₁ and E₂ = Young's modulus along direction 1 and 2

G₁₂, G₁₃, and G₂₃ = Shear modulus in 1-2 plane, 1-3 plane, and 2-3 plane

Nu₁₂ = Shear modulus

A numerical example of a squared design domain was considered in this study to verify the validity of the topology optimization method. In this study, topology optimization was performed under the Tosca module in Abaqus CAE software [10]. The squared design domain and the frame are simplified as planar shell elements [2]. Those elements are assigned as designated materials which material properties is in Table 2. The next pre-processing setup is within the Tosca optimization module. The strain energy and weight fraction are determined as design responses. While the weight fraction is determined as a constraint design response, which produced a light yet strong structure, the goal of this topology optimization is to minimize the strain energy in order to improve structural integrity. In this work, the initial failure of the frame structure is investigated using the Hashin damage criterion.

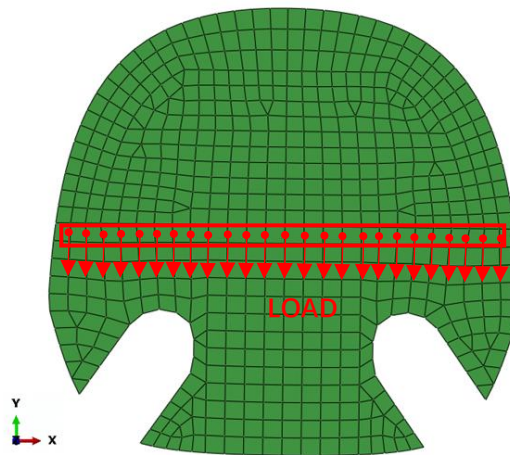


Figure 3. Frame with 50 mesh size.

Areas that have contact with another component (i.e Bottom girder, Longeron, stringer, deck, and skin) are frozen, which means those areas will not be optimized during the process. In order that, those components still have a place to attach to the frame. The frame has a mesh size of 50 with quad-only preferred elements, but in a certain area with narrow-angle geometry, the tria elements are applied. In this paper, the meshed frame structure used for the calculations and load subjected to frame structure depicted in Figure 3. The loads for topology optimization are generated by component mass distribution. Meanwhile, for ply failure prediction, the loads are subjected as a variable which will be investigated when the first failure occurred. The edge of the frame structures that have contact with fuselage skin are set to be boundary conditions.

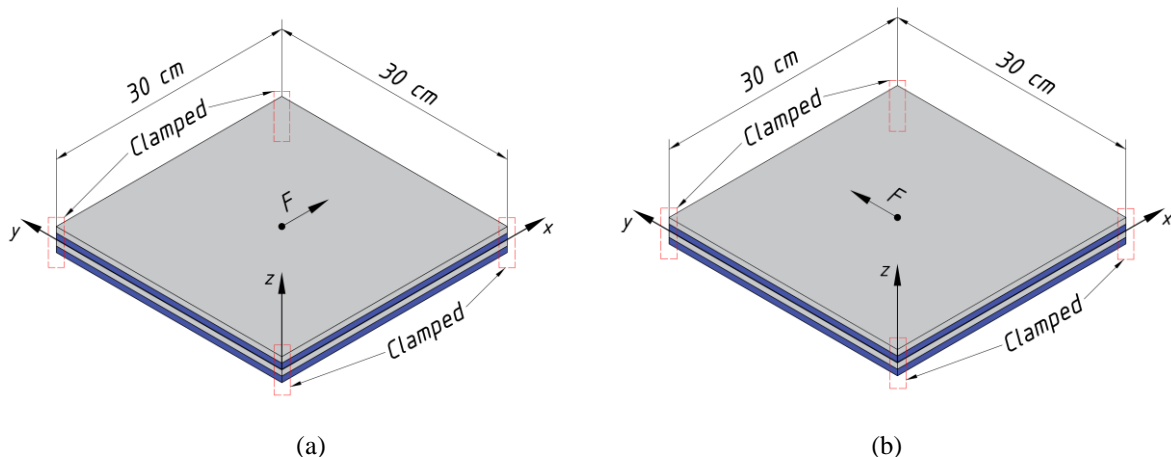


Figure 4. Setup of squared design domain (a) X-direction and (b) Y-direction [8]

RESULTS AND DISCUSSION

Benchmarking

The benchmarking phase was performed as a standard in the topology optimization process. Figure 4 shows the setup of a squared design domain which is clamped on every four corners [8]. A concentrated force with a magnitude of 8000 N was applied in the middle of the plane in the X and Y direction. A squared design domain of $300 \times 300 \times 50$ mm meshed with an element size of 4.28, which caused the design domain to be discretized with 4900 standard square plane stress elements. The mechanical properties of material used in calculations are listed as $E_1 = 132$ GPa, $E_2 = E_3 = 10.8$ GPa, $G_{12} = G_{13} = 5.65$ GPa, $G_{23} = 3.38$ GPa, $\nu_{12} = \nu_{13} = 0.24$, $\nu_{23} = 0.59$ [8].

Figure 5 shows the results of the validation process of a squared design domain. The black and white images are the results from reference literature [8], meanwhile the blue ones are the results of validation process conducted in this study. The minimum strain energy under the given loading condition (X and Y direction) was set as an objective design response. As for the optimization constraint, a weight fraction of the initial value was set to the value of 0.4. The results of the validation process show a promising result with the current optimization study. The optimization topology for a benchmark of squared design domain in X and Y direction was completed in 25 and 20 cycles, respectively.

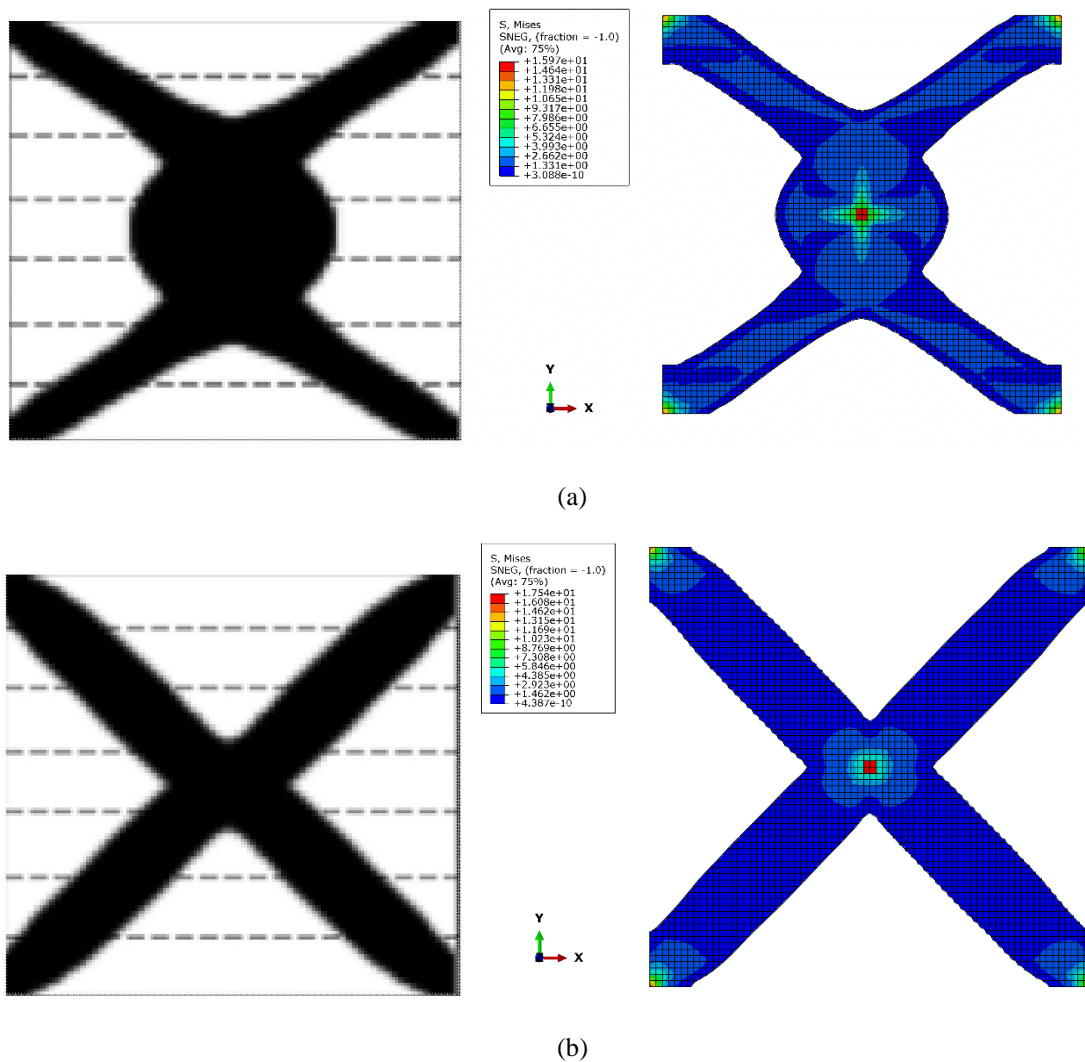


Figure 5. Results of validation process compared to the previous study [8]: (a) load in X direction and (b) load in Y direction.

Topology Optimization

The frame design model was optimized using the same method as a benchmark model squared design domain to obtain the new model which has lightweight whilst maintaining its structural integrity. To achieve the strong characteristic, a frame design was assigned to have a constraint of 50% weight and minimum strain energy. The topology optimization for frame design was completed in 33 cycles. The optimization process stops when the minimum strain energy is achieved and converged. The optimization topology process for frame shows in Figure 6.

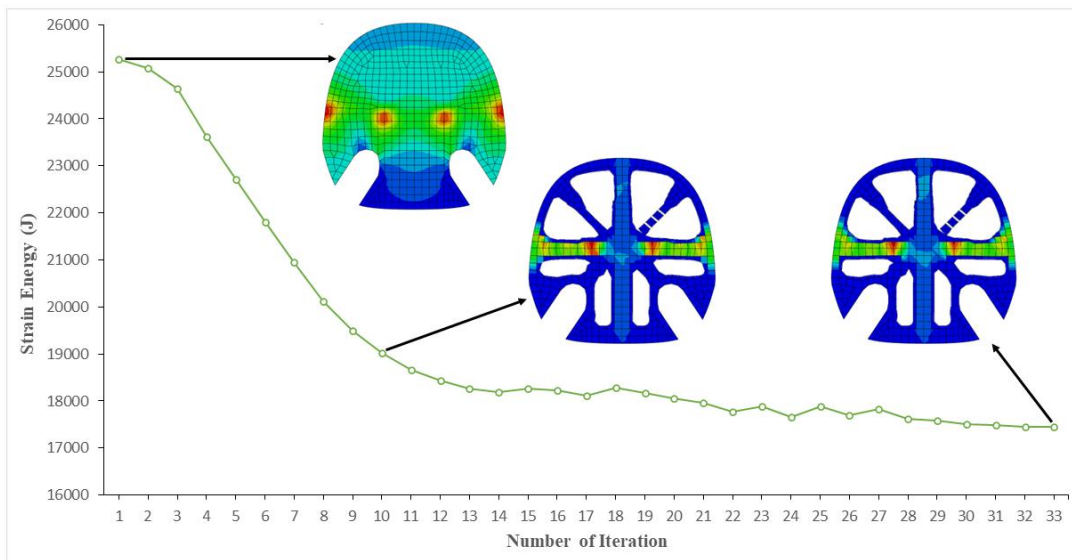


Figure 6. Topology optimization process

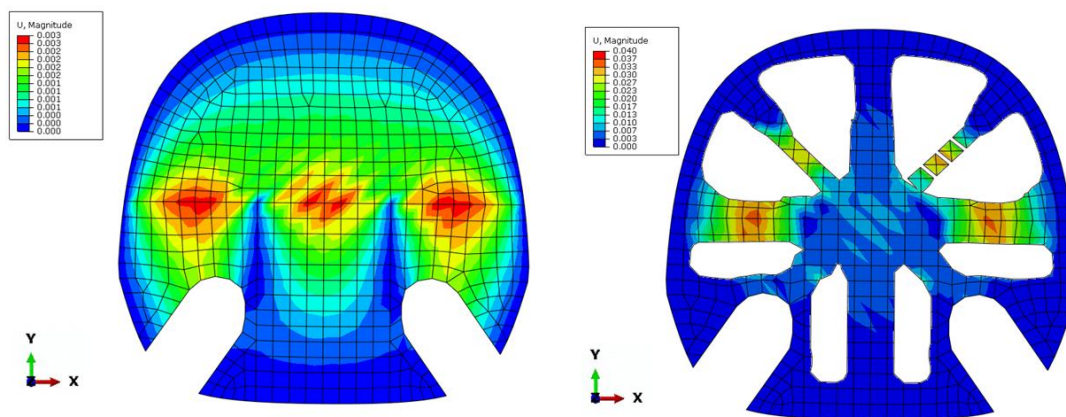
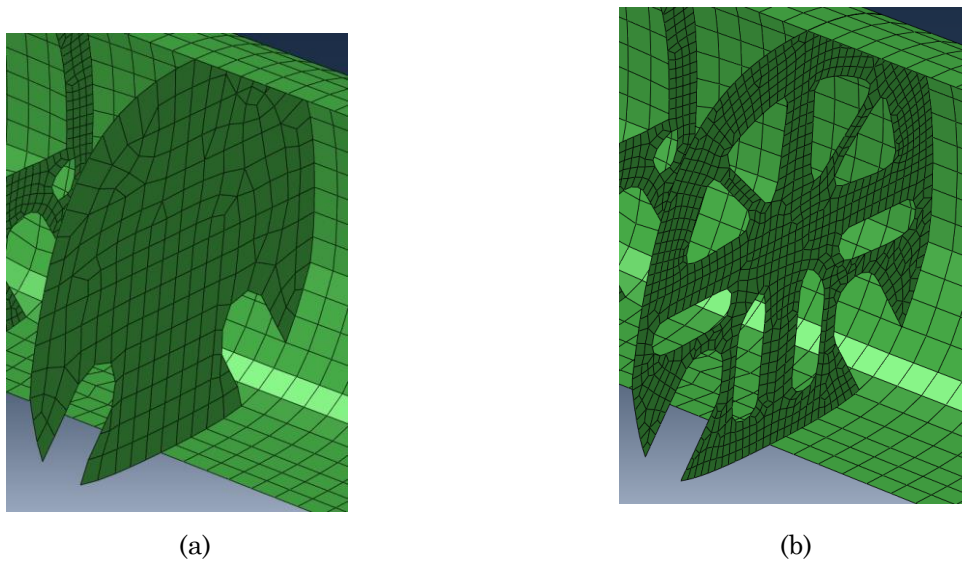


Figure 7. Magnitude of displacement



Total weight loss: 34%

Figure 8. Frame assembly before and after topology optimization: (a) initial frame 1.688 kg and (b) refined model 1.107 kg.

At the beginning of the optimization, the frame design has 25,260 joules of strain energy. Since the objective of this method is to minimize the strain energy, the final results show 17,422 joules of strain energy with some topological changes. It is also known from these studies, the magnitude of displacement (U) after the optimization process is 0.04 mm compared to its initial shape which has 0.003 mm and can be seen in Figure 7. The increased magnitude displacement is still tolerable since most of the carbon fiber has a maximum displacement of 0.7–2.4 mm [13].

The optimization has successfully reduced the weight of the frame by removing areas apart from the frozen area. Furthermore, the new model was refined using CAD software, called CATIA, due to its manufacturability. Initial weight of frame structure is 1.688 kg. After the topology optimization, the new refined model shows great improvement which has 1.107 kg of weight. The design constraint for this study is to reduce 50% of its weight, however, the optimization process managed to reduce 34% of weight to achieve the minimum strain energy possible. Therefore, 0.581 kg of weight has dissipated from this frame. Figure 8 shows a meshed frame installed in a global airframe structure.

First Failure Prediction

After the topology optimization, the process continued to the first failure prediction using Hashin criterion. Various values of load are applied to the new model to investigate the maximum load of this structure right before failure. There are four criteria used in Abaqus, Hashin's fiber tensile damage initiation criterion (HSNFCCRT), Hashin's fiber compressive damage initiation criterion (HSNFCCRT), Hashin's matrix tensile damage initiation criterion (HSNMTCRT), and Hashin's matrix compressive damage initiation criterion (HSNMTCRT). The load applied to the structure starts from 1000 N with an increment of 1000 N. The results of those four criteria are shown in Figure 9. The structure starts to fail when the Hashin criteria reach the value of 1 [2]. From Figure 9, it is known that HSNMTCRT reached the value of 1 at 9000 N, which means the first failure of the structure occurred in matrix with tensile loading conditions. On further investigation, it is known that the failure occurred in the matrix of Ply-2. The failure is located at the corner above the load nodes, which can be seen in Figure 10.

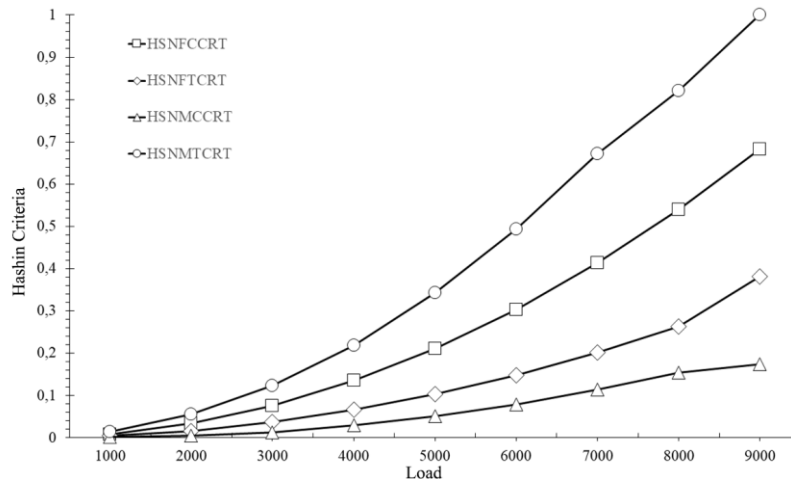


Figure 9. Frame structure's Hashin criterion

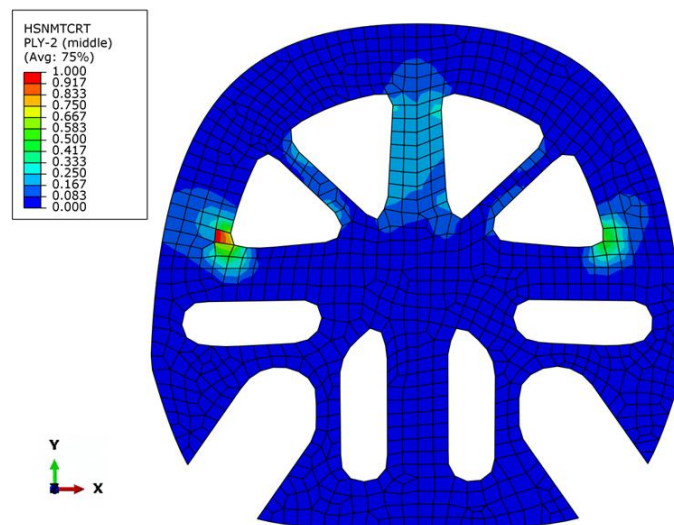


Figure 10. Frame structure matrix tensile failure

CONCLUSION

The topology optimization of MALE UAV structure has been successfully conducted. The topology optimization process in this study was carried out using a finite element method software, Abaqus. The material characteristic values of the carbon fiber laminate were modeled into one surface in a numerical domain. A benchmark is done beforehand as an attempt to validate the method used in this study by referring to previously conducted studies. The validation result shows that the method used in this study was feasible to use.

The topology optimization process of the structure design was converged at 33th iteration. The results of topology optimization show a decrease in strain energy from 25,260 Joules to 17,422 Joules and a reduction in the weight of the structure up to 0.581 kg or 34% of the initial structure weight. In addition, the result of the optimization shows an increase in displacement (U), from 0.003 mm to 0.004 mm. First failure prediction using Hashin's criterion has been successfully conducted. It is known that the first failure occurred in matrix of Ply-2 at 9000 N. It is recommended to consider the manufacturability of the structure while optimizing it for future studies.

ACKNOWLEDGEMENT

This work is supported by the project of "Topology optimization of MALE UAV fuselage structure with numerical approach based on finite element method" No.6/III/HK/2022 under the grant of Research Organization for Aeronautics and Space of National Research and Innovation Agency (BRIN), Bogor, Indonesia.

REFERENCES

- [1] J. Zhu, H. Zhou, C. Wang, L. Zhou, S. Yuan, and W. Zhang. "A review of topology optimization for additive manufacturing: status and challenges." *Chinese Journal of Aeronautics*, vol. 34, pp. 91-110, Jan. 2021.
- [2] N. Bencherif and M. Benhaliliba. "A Hashin Criteria Investigation to Predict the Interaction Effect of Defaults on the Damage of Composite Pipe." *Oriental Journal of Chemistry*, vol. 37, no. 2, pp. 314-320, Mar. 2021.
- [3] T. L. Htet and P. V. Prosuntsov. "Parametric and Topology Optimization of Polymer Composite Load Bearing Elements of Rear Part of Aircraft Fuselage Structure," in *AIP Conference Proceedings 2318*, 2021, p. 020008.
- [4] L. Iqbal and J. Sullivan. "Comprehensive aircraft preliminary design methodology applied to the design of MALE UAV," in *47th AIAA Aerosp. Sci. Meet. New Horiz. Forum Aerosp. Expo*, 2009, pp. 431. s
- [5] Y. Lu and L. Tong. "Concurrent optimization of topologies and fiber orientations for laminated composite structures." *Composite Structures*, vol. 295, p. 115749, Sep. 2022.
- [6] D. Harvey and P. Hubert. "3D topology optimization of sandwich structures with anisotropic shells." *Composite Structures*, vol. 285, p. 115237, Apr. 2022.
- [7] E. Karachalios, K. Munoz, M. Jimenez, V. Prentzias, S. Goossens, T. Geernaert, and T. S. Plagianakos. "LRI-fabricated composite demonstrators for an aircraft fuselage on the basis of a building block design approach." *Composite Part C: Open Access*, vol. 6, p. 100178, Oct. 2021.
- [8] J. W. Lee, J. J. Kim, H. S. Kim, and G. H. Yoon. "Application of a layerwise theory for efficient topology optimization of laminate structure." *Journal of Mechanical Science and Technology*, vol. 33, no. 2, pp. 711-719. 2019.
- [9] E. J. Barbero and M. Shahbazi. "Determination of Material Properties for ANSYS Progressive Damage Analysis of Laminated Composites." *Composite Structures*, vol. 176, pp. 768-779. 2017.
- [10] ABAQUS (2021). *Analysis User's Manual, Version 6.23* [Online]. Available: <https://www.3ds.com/products-services/simulia/products/abaqus/>
- [11] J. Pederson. "Finite Element Analysis of Carbon Composite Ripping using Abaqus". M. Sc. theses, Clemson University, US, 2006.
- [12] Hexcel Corporation (2022). *Hexcel is a global leader in advanced composites technology* [Online]. Available: www.hexcel.com.
- [13] C. Elanchezian, B. Vijaya Ramnath, J. Hemalatha, [2014], "Mechanical behaviour of glass and carbon fibre reinforced composites at varying strain rates and temperatures." *Procedia Materials Science*, vol. 6, pp. 1405-1418. 2014.

